Thermodynamic geometry and thermal stability of n-dimensional dilaton black holes in the presence of logarithmic nonlinear electrodynamics

A. Sheykhi,[1,2,*] F. Naeimipour,[1] and S. M. Zebarjad[1,†]

[1]*Physics Department and Biruni Observatory, College of Sciences, Shiraz University, Shiraz 71454, Iran*
[2]*Research Institute for Astronomy and Astrophysics of Maragha (RIAAM), P.O. Box 55134-441 Maragha, Iran*

(Received 1 October 2015; published 23 December 2015)

In this paper, we construct a new class of black hole solutions which is coupled to the logarithmic nonlinear electrodynamics in the context of dilaton gravity. We consider an n-dimensional action in which gravity is coupled to the logarithmic nonlinear electrodynamics field and a scalar dilaton field to obtain the equations of motion of the gravitational, dilaton and electromagnetic fields. This leads to finding a new class of n-dimensional static and spherically symmetric black hole solutions in the presence of two Liouville-type dilaton potentials. The asymptotic behavior of these solutions is neither flat nor (anti-)de Sitter [(A)dS], and in the limiting case where the nonlinear parameter β goes to infinity, our solutions reduce to the black holes of Einstein-Maxwell-dilaton gravity in higher dimensions. Thermodynamic quantities such as mass, temperature, electric potential and entropy are also computed, and it is shown that they agree with the first law of thermodynamics. Furthermore, we find that for small values of the electric charge parameter q, and the dilaton coupling constant α, as well as small dimension n, the solutions are thermally stable. By increasing n, the region of stability stands for smaller values of α independent of q. Finally, we use the method of thermodynamical geometry and find the phase transition points by calculating the Ricci scalar of a thermodynamic metric.

DOI: 10.1103/PhysRevD.92.124054 PACS numbers: 04.70.Bw, 04.30.-w, 04.70.-s, 04.70.Dy

I. INTRODUCTION

Classical linear Maxwell electrodynamics with charged pointlike particles has two limited properties. First, the electromagnetic energy of a pointlike particle diverges at its location. Second, the Lorentz force must be postulated to describe interactions between pointlike particles and the electromagnetic field. Nonlinear vacuum electrodynamics is free of these imperfections. The theory of nonlinear electrodynamics was first introduced in the 1930s by Born and Infeld (BI) [1]. Their purpose was to obtain a classical theory of charged particles with finite self-energy by introducing an upper bound for the electric field at the origin [1]. BI theory has received a lot of attention because it has applications to the description of D-branes, mostly in the context of type-IIB string theory and to the AdS/CFT correspondence [2,3]. However, the BI theory is not the only nonlinear electrodynamics theory proposed so far. In recent years, other types of nonlinear electrodynamics, such as exponential [4], power law [5] and logarithmic [6], were proposed. It is worth mentioning that the logarithmic form of the electrodynamic Lagrangian, like BI electrodynamics, removes divergences in the electric field, while the exponential form of the nonlinear electromagnetic field does not cancel the divergency of the electric field at $r = 0$; however, its singularity is much weaker than Einstein-Maxwell theory.

On the other side, the idea of dilaton gravity has received a lot of attention because of its close connection with the low-energy limit of string theory. The low-energy limit of string theory leads to Einstein gravity, coupled nonminimally to a scalar dilaton field, which is massless in all finite orders of perturbation theory [7]. In fact, in order to avoid conflict with classical tests of the tensor character of gravity, the physical dilaton should have mass. Some classes of black hole solutions have been found for massive dilatons [8–10]. At the classical level, and at distance scales small compared to the dilaton Compton wavelength, we can neglect the mass and study the effect of the dilaton on low-energy physics. In this theory, neutral black holes are still described by the Schwarzschild metric, and the scalar dilaton plays no role. For charged black holes, however, the dilaton plays a crucial role in modifying the causal structure of the solutions. The studies on the dilaton black holes have been carried out in various aspects (see, e.g., Refs. [11–13] and references therein).

Four-dimensional black holes have a number of remarkable properties. It is natural to ask whether these properties are general features of black holes or whether they crucially depend on the world being four dimensional. There are several motivations for studying higher-dimensional black holes. The first originates from string theory, which is a promising approach to quantum gravity. String theory predicts that spacetime has more than four dimensions

*asheykhi@shirazu.ac.ir
†zebarjad@susc.ac.ir

[14,15]. Another reason originates from the AdS/CFT correspondence, which relates the properties of an n-dimensional black hole with those of a quantum field theory in $(n-1)$ dimensions [16]. Considering these facts, we have enough motivation to investigate the higher-dimensional logarithmic nonlinear (LN) electrodynamics in the presence of the scalar dilaton field. Previously, n-dimensional black hole solutions of BI theory coupled to the dilaton field (BId) [17–26], exponential nonlinear electrodynamics coupled to the dilaton field (ENd) [27], and the power-law Maxwell field in the presence of the dilaton field [28] have been constructed, and their thermodynamics have also been explored.

In this paper, we would like to fill in the gap existing in the literature by investigating the n-dimensional black hole solutions of LN theory in the presence of the scalar dilaton field (LNd). The Lagrangian of this theory, in four dimensions, was previously introduced, and its exact black hole solutions, as well as their thermodynamics, were explored [29]. Here, we would like to generalize the four-dimensional LNd solutions [29] to all higher dimensions. The suitable Lagrangian has the following form:

$$L_{\mathrm{LNd}}(F,\Phi) = -8\beta^2 e^{4\alpha\Phi/(n-2)} \times \ln\left(1+\frac{e^{-8\alpha\Phi/(n-2)}F^2}{8\beta^2}\right), \tag{1}$$

where Φ is the dilaton field, $F^2 = F_{\mu\nu}F^{\mu\nu}$, $F_{\mu\nu} = \partial_{[\mu}A_{\nu]}$ is the electromagnetic field tensor, and A_μ is the electromagnetic potential. The constant α measures the strength of the coupling of the scalar and electromagnetic field, while β is the nonlinear parameter with dimension of mass. In the absence of the dilaton field ($\alpha = 0$) and in four dimensions where $n = 4$, $L(F,\Phi)$ reduces to the LN electrodynamic Lagrangian presented in [6]. The series expansion of (1) for large β leads to

$$L_{\mathrm{LNd}}(F,\Phi) = -e^{-4\alpha\Phi/(n-2)}F^2 + \frac{e^{-12\alpha\Phi/(n-2)}F^4}{16\beta^2} - \frac{e^{-20\alpha\Phi/(n-2)}F^6}{192\beta^4} + \mathcal{O}\left(\frac{1}{\beta^6}\right). \tag{2}$$

One of the criterion for choosing different kinds of nonlinear electrodynamics is that they have the same expansion for large β. Indeed, the series expansion of two nonlinear Lagrangians, namely, BId DHSR and ENd [27], have the same form as (2),

$$L_{\mathrm{BId}}(F,\Phi) = -e^{-4\alpha\Phi/(n-2)}F^2 + \frac{e^{-12\alpha\Phi/(n-2)}F^4}{8\beta^2} - \frac{e^{-20\alpha\Phi/(n-2)}F^6}{32\beta^4} + \mathcal{O}\left(\frac{1}{\beta^6}\right), \tag{3}$$

$$L_{\mathrm{ENd}}(F,\Phi) = -e^{-4\alpha\Phi/(n-2)}F^2 + \frac{e^{-12\alpha\Phi/(n-2)}F^4}{8\beta^2} - \frac{e^{-20\alpha\Phi/(n-2)}F^6}{96\beta^4} + O\left(\frac{1}{\beta^6}\right). \tag{4}$$

Comparing the series expansions given in (2), (3) and (4), we see that all of them have the same behavior up to a coefficient number. For $\beta \to \infty$, all of these Lagrangians reduce to the standard linear Maxwell Lagrangian coupled to the dilaton field in n dimensions, $-e^{-4\alpha\Phi/(n-2)}F^2$ [30,31]. This is an expected result, since in the limit of large β, these nonlinear theories should recover the Einstein-Maxwell-dilaton (EMd) theory.

For the above mentioned, the investigation on the black hole spacetimes in the framework of LNd theory is of great importance. In the present work, by considering two Liouville potentials for the dilaton field and making a suitable *ansatz*, we construct a new class of n-dimensional black hole solutions in the framework of LNd theory (1). We also investigate the physical properties of the spacetime and explore thermodynamics and thermal stability, as well as thermodynamic geometry of the obtained solutions. Throughout this paper, we work in natural units and set $\hbar = c = G = k_B = 1$.

This paper is organized as follows. In Sec. II, we introduce the n-dimensional action in which gravity is coupled to the dilaton and EN electrodynamics. Then, we vary the action to obtain the corresponding field equations. By taking the suitable *ansatz*, we construct a new class of static and spherically symmetric black hole solutions of this theory. In Sec. III, we investigate the physical properties as well as the structure of the obtained solutions. In Sec. IV, we study thermodynamics of higher-dimensional dilaton black holes in the presence of nonlinear electrodynamics and check the validity of the first law of thermodynamics. In Secs. V and VI, we study thermal stability of the obtained solutions in canonical and grand-canonical ensembles, respectively. Using the thermodynamic geometry approach, we study the phase transition points in Sec. VII. We finish our paper with some concluding remarks in Sec. VIII.

II. FIELD EQUATIONS AND BLACK HOLE SOLUTIONS

We consider the n-dimensional ($n \geq 4$) action in which gravity is coupled to the dilaton and nonlinear electrodynamic fields,

$$S = \frac{1}{16\pi}\int d^n x\sqrt{-g}\left(\mathcal{R} - \frac{4}{n-2}(\nabla\Phi)^2 - V(\Phi) + L_{\mathrm{LNd}}(F,\Phi)\right), \tag{5}$$

where $\mathcal{R}$ and $V(\Phi)$ are, respectively, the Ricci scalar curvature and the dilaton potential. We take the potential of the dilaton field as

$$V(\Phi) = 2\Lambda_0 e^{2\zeta_0\Phi} + 2\Lambda e^{2\zeta\Phi}. \tag{6}$$

The dilaton potential has two Liouville terms in which Λ_0, Λ, ζ_0 and ζ are constants. This kind of potential has been studied in the context of BId black holes [24,25] as well as EMd gravity [30–34]. Our purpose in this paper is to study LN electrodynamics coupled to the scalar dilaton field in n-dimensional spacetime. First of all, for simplification, we write $L_{\rm LNd}(F,\phi)$ as

$$L_{\rm LNd}(F,\Phi) = -8\beta^2 e^{4\alpha\Phi/(n-2)}\mathcal{L}(Y), \tag{7}$$

where we have defined

$$\mathcal{L}(Y) = \ln(1+\mathrm{Y}), \tag{8}$$

$$Y = \frac{e^{-8\alpha\Phi/(n-2)}F^2}{8\beta^2}. \tag{9}$$

Varying action (5) with respect to the gravitational field $g_{\mu\nu}$, the dilaton field Φ and the electromagnetic field A_μ, we have

$$\begin{aligned}\mathcal{R}_{\mu\nu} = {}& \frac{4}{n-2}\left(\partial_\mu\Phi\partial_\nu\Phi + \frac{1}{4}g_{\mu\nu}V(\Phi)\right) \\ & + 2e^{-4\alpha\Phi/(n-2)}\partial_Y\mathcal{L}(Y)F_{\mu\eta}F_\nu{}^\eta \\ & - \frac{8\beta^2}{n-2}e^{4\alpha\Phi/(n-2)}[2Y\partial_Y\mathcal{L}(Y) - \mathcal{L}(Y)]g_{\mu\nu},\end{aligned} \tag{10}$$

$$\nabla^2\Phi = \frac{n-2}{8}\frac{\partial V}{\partial\Phi} - 4\alpha\beta^2 e^{4\alpha\Phi/(n-2)}[2Y\partial_Y\mathcal{L}(Y) - \mathcal{L}(Y)], \tag{11}$$

$$\nabla_\mu(e^{-4\alpha\Phi/(n-2)}\partial_Y\mathcal{L}(Y)F^{\mu\nu}) = 0. \tag{12}$$

In the limit of linear electrodynamics ($\beta^2\to\infty$), we have $\mathcal{L}(Y) = Y$, and the system of equations restores those of EMd theory [30–34].

We would like to search for the static and spherically symmetric solutions of the field equations (10)–(12). The proper metric for the spacetime of these solutions is

$$ds^2 = -f(r)dt^2 + \frac{dr^2}{f(r)} + r^2R^2(r)d\Omega^2_{n-2}, \tag{13}$$

where $f(r)$ and $R(r)$ are functions of r and we should gain them. Here, $d\Omega^2_{n-2}$ denotes the metric of a unit $(n-2)$-sphere. In the absence of a dilaton field ($\alpha = 0$), we have $R(r) = 1$. Using the metric (5), we try to solve the field equations (10)–(12). First, we solve the electromagnetic field equation (12) to find $F_{\mu\nu}$. We assume all components of $F_{\mu\nu}$ are zero, except F_{tr}. Integrating Eq. (12), we obtain F_{tr} as

$$F_{\rm tr} = \frac{2qe^{4\alpha\Phi/(n-2)}}{(rR(r))^{n-2}}\left(1+\sqrt{1+\frac{q^2}{\beta^2(rR(r))^{2n-4}}}\right)^{-1}, \tag{14}$$

where q, an integration constant, is the charge parameter. In the limiting case where $\beta\to\infty$, Eq. (14) reduces to

$$F_{\rm tr} = \frac{qe^{4\alpha\Phi/(n-2)}}{(rR(r))^{n-2}} + \mathcal{O}\left(\frac{1}{\beta^2}\right). \tag{15}$$

This expression is the electric field of an n-dimensional EMd black hole [31]. In the absence of the dilaton field and for $n = 4$, Eq. (14) recovers [35]

$$F_{\rm tr} = \frac{2q}{r^2}\left(1+\sqrt{1+\frac{q^2}{\beta^2r^4}}\right)^{-1}. \tag{16}$$

For other unknown functions $f(r)$, $R(r)$ and $\Phi(r)$, we should solve the field equations (10) and (11). In order to obtain these functions, we make the *ansatz*

$$R(r) = e^{2\alpha\Phi/(n-2)}. \tag{17}$$

This *ansatz* was first introduced in [36] for the purpose of finding black string solutions of EMd gravity, and later was applied for constructing black hole solutions of nonlinear BId theory [25]. The mentioned *ansatz* is according to our expectation; namely, in the absence of a dilaton field ($\alpha = 0$), it recovers $R(r) = 1$. Using the *ansatz* (17), the metric (13) and the electric field (14), we can solve the gravitational and dilaton field equations (10) and (11). We find

$$\begin{aligned}f(r) = {}& -\frac{(n-3)(\alpha^2+1)^2}{(\alpha^2-1)(\alpha^2+n-3)}b^{-\gamma}r^\gamma - \frac{m}{r^{n-3-(n-2)\gamma/2}} \\ & + \frac{2(\alpha^2+1)^2(\Lambda-4\beta^2)b^\gamma}{(n-2)(\alpha^2-n+1)}r^{2-\gamma} \\ & - \frac{8\beta^2(\alpha^2+1)b^\gamma}{(n-2)r^{n-3-(n-2)\gamma/2}} \\ & \times\int r^{n(1-\frac{\gamma}{2})-2}\left\{\sqrt{1+\eta} - \ln\left(\frac{\eta}{2}\right)\right. \\ & \left. + \ln\left(-1+\sqrt{1+\eta}\right)\right\}dr,\end{aligned} \tag{18}$$

$$\Phi(r) = \frac{(n-2)\alpha}{2(\alpha^2+1)}\ln\left(\frac{b}{r}\right), \tag{19}$$

where m and b are integration constants and

$$\gamma = \frac{2\alpha^2}{1+\alpha^2}, \tag{20}$$

$$\eta = \frac{q^2 b^{(2-n)\gamma}}{\beta^2 r^{(n-2)(2-\gamma)}}. \tag{21}$$

The above solutions will fully satisfy all components of the field equations provided we choose

$$\zeta_0 = \frac{2}{\alpha(n-2)}, \tag{22}$$

$$\zeta = \frac{2\alpha}{n-2}, \tag{23}$$

$$\Lambda_0 = \frac{(n-2)(n-3)\alpha^2}{2b^2(\alpha^2-1)}. \tag{24}$$

In relation (18), Λ is a free parameter which plays the role of the cosmological constant. We can redefine it as usual, $\Lambda = -(n-1)(n-2)/2l^2$, where l is a constant with dimension of length. By solving the integration in relation (18), we have

$$\begin{aligned} f(r) = &-\frac{(n-3)(\alpha^2+1)^2}{(\alpha^2-1)(\alpha^2+n-3)} b^{-\gamma} r^{\gamma} - \frac{m}{r^{n-3-(n-2)\gamma/2}} + \frac{2(\Lambda-4\beta^2)(\alpha^2+1)^2 b^{\gamma}}{(n-2)(\alpha^2-n+1)} r^{2-\gamma} \\ &+ \frac{8\beta^2(\alpha^2+1)^2}{(\alpha^2-n+1)^2} b^{\gamma} r^{2-\gamma} \left\{ 1 - {}_2F_1\left(\left[\frac{-1}{2}, \frac{\alpha^2-n+1}{2n-4} \right], \left[\frac{\alpha^2+n-3}{2n-4} \right], -\eta \right) \right\} \\ &+ \frac{8\beta^2(\alpha^2+1)^2}{(n-2)(\alpha^2-n+1)} b^{\gamma} r^{2-\gamma} \left\{ \sqrt{1+\eta} - \ln\left(\frac{\eta}{2}\right) + \ln\left(-1+\sqrt{1+\eta}\right) \right\}, \end{aligned} \tag{25}$$

where ${}_2F_1([a,b],[c],d)$ is the hypergeometric function [37]. It is worth mentioning that the solutions are ill defined for $\alpha = 1$ and $\alpha = \sqrt{n-1}$. We expect that for large β, the function $f(r)$ reduces to the obtained solution of higher-dimensional black holes in EMd gravity [31]. Indeed, if we expand (25) for large β, we arrive at

$$\begin{aligned} f(r) = &-\frac{(n-3)(\alpha^2+1)^2}{(\alpha^2-1)(\alpha^2+n-3)} b^{-\gamma} r^{\gamma} - \frac{m}{r^{n-3-(n-2)\gamma/2}} \\ &+ \frac{2\Lambda(\alpha^2+1)^2}{(n-2)(\alpha^2-n+1)} b^{\gamma} r^{2-\gamma} \\ &+ \frac{2q^2(\alpha^2+1)^2 b^{-(n-3)\gamma}}{(n-2)(\alpha^2+n-3) r^{(n-3)(2-\gamma)}} \\ &- \frac{q^4(\alpha^2+1)^2 b^{-(2n-5)\gamma}}{4\beta^2(n-2)(\alpha^2+3n-7) r^{(2n-5)(2-\gamma)}} + \mathcal{O}\left(\frac{1}{\beta^4}\right). \end{aligned} \tag{26}$$

Setting $\alpha = \gamma = 0$ in (26), we reach

$$\begin{aligned} f(r) = 1 &- \frac{m}{r^{n-3}} + \frac{r^2}{l^2} + \frac{2q^2}{(n-2)(n-3) r^{2n-6}} \\ &- \frac{1}{4\beta^2(n-2)(3n-7)} \frac{q^4}{r^{4n-10}} + \mathcal{O}\left(\frac{1}{\beta^4}\right), \end{aligned} \tag{27}$$

which has the form of static, spherically symmetric, n-dimensional Reissner-Nordstrom (RN) black holes in AdS spacetime in the limit $\beta \to \infty$. The last term in the right-hand side of (27) is the leading nonlinear correction term to the RN-AdS black hole in the large β limit. It is interesting to investigate the asymptotic behavior of the obtained solutions. From Eq. (26), one can easily see that in the presence of the dilaton field, the asymptotic behavior of the solution is neither flat nor AdS. Let us explicitly write the large r limit of $f(r)$,

$$\begin{aligned} \lim_{r\to\infty} f(r) = &-\frac{(n-3)(\alpha^2+1)^2}{(\alpha^2-1)(\alpha^2+n-3)} b^{-\gamma} r^{\gamma} \\ &+ \frac{2\Lambda(\alpha^2+1)^2}{(n-2)(\alpha^2-n+1)} b^{\gamma} r^{2-\gamma}. \end{aligned} \tag{28}$$

For example, if we take $\alpha = \sqrt{2}$, $n = 6$ and $b = 1$, we find

$$\lim_{r\to\infty} f(r) = -\frac{27}{5} r^{4/3} - \frac{3\Lambda}{2} r^{2/3}. \tag{29}$$

Clearly, the metric function (29) is neither flat nor (A)dS. Indeed, it has been shown that no dilaton dS or AdS black hole solution exists with the presence of only one or two Liouville-type dilaton potentials [13]. In the presence of one or two Liouville-type potentials, black hole spacetimes which are neither asymptotically flat nor (A)dS have been explored by many authors (see, e.g., Refs. [30–34]). It is important to note that this asymptotic behavior is not due to the nonlinear nature of the electrodynamic field, since as $r \to \infty$ the effects of the nonlinearity disappear. This is due to the fact that the $r \to \infty$ limit corresponds to $\beta^2 \to \infty$, and in this case F_{tr}, as well as the metric functions $f(r)$, restore the results of EMd with an unusual asymptotic [31].

III. PHYSICAL PROPERTIES OF THE SOLUTIONS

Now, we investigate the physical properties of the solutions. As we mentioned in the Introduction, one of the main purposes for introducing the nonlinear electrodynamics is to remove the singularity of the electric field at the origin. So, to check the correction of the corresponding nonlinear theory, we should investigate whether this theory could remove this divergency or not. To have a better understanding of the behavior of the electric field, we plot $E(r)$ versus r for different values of the parameters. Replacing (19) and (17) in (14), we have

$$F_{\rm tr} = E(r) = \frac{2qb^{(4-n)\gamma/2}}{r^{n-2+2\gamma-n\gamma/2}}\left[1+\sqrt{1+\frac{q^2b^{-(n-2)\gamma}}{\beta^2 r^{(n-2)(2-\gamma)}}}\right]^{-1}. \tag{30}$$

Expanding for large β, we get

$$E(r) = \frac{qb^{(4-n)\gamma/2}}{r^{n-2+(4-n)\gamma/2}} - \frac{q^3}{4\beta^2}\frac{b^{\gamma(4-3n/2)}}{r^{3n-6+\gamma(4-3n/2)}} + \frac{q^5}{8\beta^4}\frac{b^{\gamma(6-5n/2)}}{r^{5n-10+\gamma(6-5n/2)}} + \mathcal{O}\left(\frac{1}{\beta^6}\right). \tag{31}$$

We have plotted the behavior of $E(r)$ versus r in Figs. 1–5. The similar characteristic of all figures is that for large r, $E(r)$ goes to zero independent of the values of the other parameters. Figure 1 shows the effects of the dilaton field on the electric field of LNd electrodynamics. As one can see from this figure, the curve $\alpha = 0$ satisfies our expectation and the electric field is finite at the origin. But in the presence of the dilaton field ($\alpha \neq 0$), $E(r)$ leads to infinity at exactly $r = 0$. So the presence of the dilaton field in this theory, like BI theory, leads to the divergency. Also, by

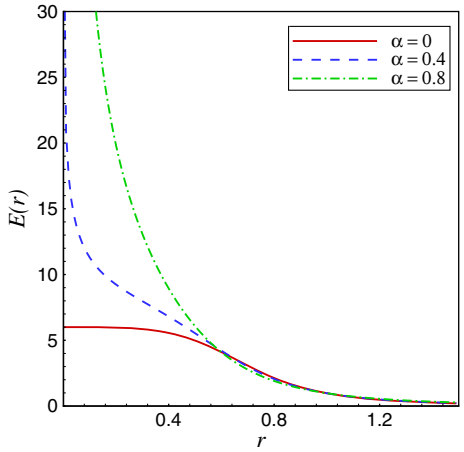

FIG. 1 (color online). The behavior of the electric field $E(r)$ of LNd black holes versus r for $b = 1$, $q = 1$, $\beta = 3$ and $n = 6$.

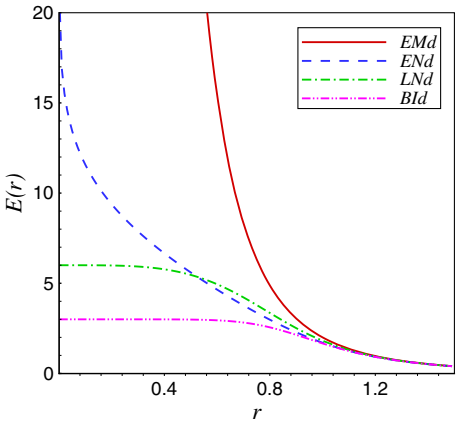

FIG. 2 (color online). The behavior of the electric field $E(r)$ versus r for EMd, ENd, LNd and BId electrodynamics for $b = 0.1$, $q = 2$, $\beta = 3$, $n = 6$ and $\alpha = 0$.

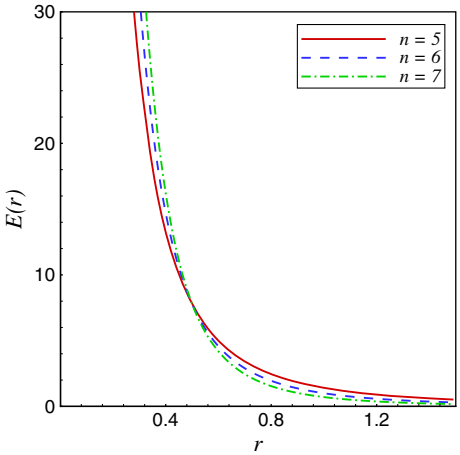

FIG. 3 (color online). The behavior of the electric field $E(r)$ of LNd black holes versus r for $\alpha = 1$, $b = 2$, $q = 2$ and $\beta = 6$.

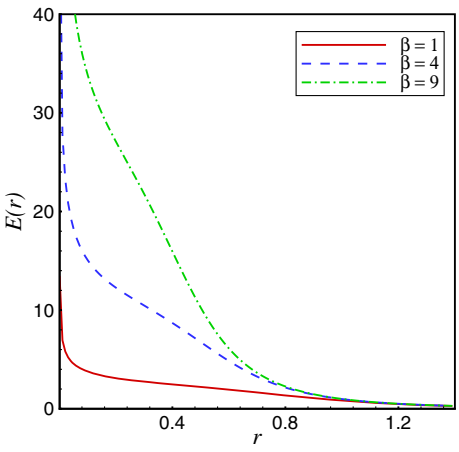

FIG. 4 (color online). The behavior of the electric field $E(r)$ of LNd black holes versus r for $b = 1$, $q = 1$, $\alpha = 0.4$ and $n = 6$.

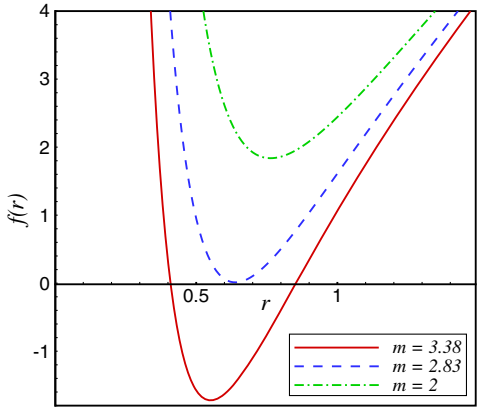

FIG. 5 (color online). $f(r)$ versus r for $\alpha = 0.5$, $q = 2$, $\beta = 1$ and $n = 6$.

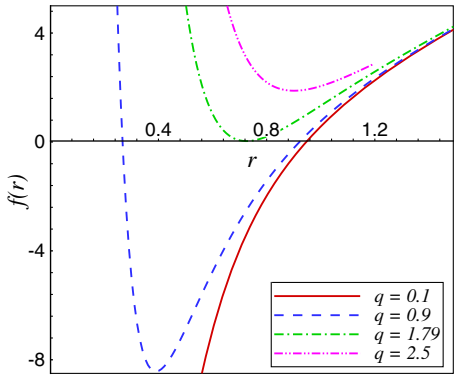

FIG. 6 (color online). $f(r)$ versus r for $\alpha = 0.5$, $m = 3$, $\beta = 4$ and $n = 6$.

increasing α, the divergency of the electric field near the origin increases.

In Fig. 2, we have compared the behavior of the electric field for EMd, BId, ENd and LNd electrodynamics in the absence of the dilaton field ($\alpha = 0$). At $r = 0$, the electric field of EMd and ENd goes to infinity but the divergency of the latter is weaker compared to the former. However, the electric fields of LNd and BId theories have finite values at $r = 0$. In Fig. 3, we have plotted the behavior of $E(r)$ of LNd for different values of dimensions. The behavior of $E(r)$ is independent of the dimension. In Fig. 4, we have plotted $E(r)$ of LNd black holes for different values of the nonlinear parameter β. As β becomes larger, the plot gets closer to the EMd and the electric field diverges as $r \to 0$. This is an expected result, since for large β, our theory reduces to the well-known EMd gravity [31].

It is important to explore the casual structure of the solutions and check whether there are the curvature singularities and horizons or not. To find the singularity of the spacetime, we should study the Kretschmann scalar $R_{\mu\nu\lambda\kappa}R^{\mu\nu\lambda\kappa}$. We find that the Kretschmann scalar diverges as $r \to 0$. Thus, the spacetime has an essential singularity located at $r = 0$. Then, we find the horizons. To find the location of the horizons of the spacetime, we should solve $f(r_+) = 0$ and obtain its roots. Because of the complex form of $f(r)$, we cannot find the locations of the horizons analytically. To have a better understanding of the nature of the horizon, we plot $f(r)$ versus r for different values of the metric parameters in Figs. 5 and 6. For simplification, we choose $l = b = 1$. Depending on the value of the metric parameters, our solutions can represent a black hole with two horizons, an extremal black hole or a naked singularity. In the case of an extremal black hole, the two horizons meet each other, and for a naked singularity, we have no horizons. For example, in Fig. 5, by decreasing the value of m (for fixed values of the other parameters), the number of horizons decreases. Also, in Fig. 6, we see that we have a $q_{\rm min}$ and a $q_{\rm ext}$ (the values of the other parameters are fixed) for which the number of horizons depends on the charge parameter q. For different values of q, we have different black holes as follows:

$$\begin{cases} q < q_{\rm min}, & \text{nonextremal black hole } (q = 0.1), \\ q_{\rm min} < q < q_{\rm ext}, & \text{black hole with two horizons } (q = 0.9), \\ q = q_{\rm ext}, & \text{extremal black hole } (q = 1.79), \\ q > q_{\rm ext}, & \text{naked singularity } (q = 2.5). \end{cases} \tag{32}$$

For a nonextremal black hole, the sign of $f(r)$ for $r > r_+$ differs from the one for $r < r_+$. Also, it is notable to mention that the values of $q_{\rm min}$ and $q_{\rm ext}$ are determined by the other parameters. The plot of mass parameter m versus r_h is also helpful for probing the horizons. By solving $f(r_h) = 0$ and finding $m(r_h)$, we can write the mass parameter as

$$\begin{aligned} m(r_h) = & -\frac{(n-3)(\alpha^2+1)^2}{(\alpha^2-1)(\alpha^2+n-3)} b^{-\gamma} r_h^{n-3-(n-4)\gamma/2} \\ & + \frac{2(\Lambda - 4\beta^2)(\alpha^2+1)^2 b^{\gamma}}{(n-2)(\alpha^2-n+1)} r_h^{n-1-n\gamma/2} \\ & + \frac{8\beta^2(\alpha^2+1)^2}{(\alpha^2-n+1)^2} b^{\gamma} r_h^{n-1-n\gamma/2} \\ & \times \left\{ 1 - {}_2F_1\left(\left[\frac{-1}{2}, \frac{\alpha^2-n+1}{2n-4} \right], \left[\frac{\alpha^2+n-3}{2n-4} \right], -\eta_h \right) \right\} \\ & + \frac{8\beta^2(\alpha^2+1)^2}{(n-2)(\alpha^2-n+1)} b^{\gamma} r_h^{n-1-n\gamma/2} \\ & \times \left\{ \sqrt{1+\eta_h} - \ln\left(\frac{\eta_h}{2} \right) + \ln\left(-1 + \sqrt{1+\eta_h} \right) \right\}, \end{aligned} \tag{33}$$

where $\eta_h = \eta(r = r_h)$. In Fig. 7, we have plotted the curve of $m(r_h)$ for the fixed values of the parameters $(\alpha = 0.8, \beta = 2, n = 7, q = 1.2)$, and the other curves are for $m(r_h) = m$, where m is constant. Again, for

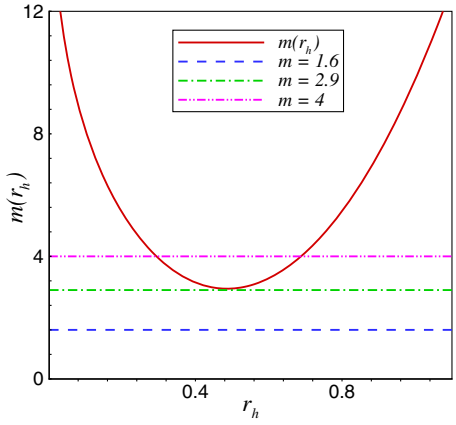

FIG. 7 (color online). The mass parameter m versus r_h for $\alpha = 0.8$, $q = 1.2$, $\beta = 2$ and $n = 7$.

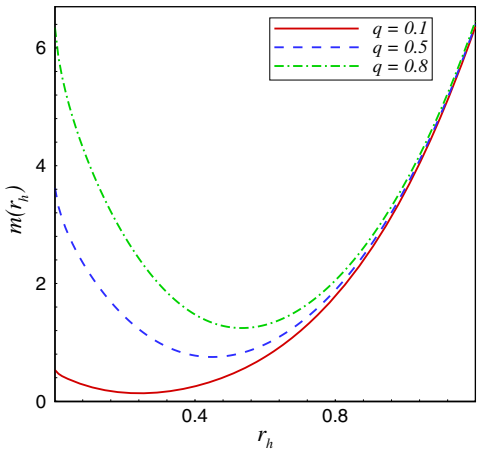

FIG. 8 (color online). The mass parameter m versus r_h for $\alpha = 0.5$, $\beta = 3$ and $n = 6$.

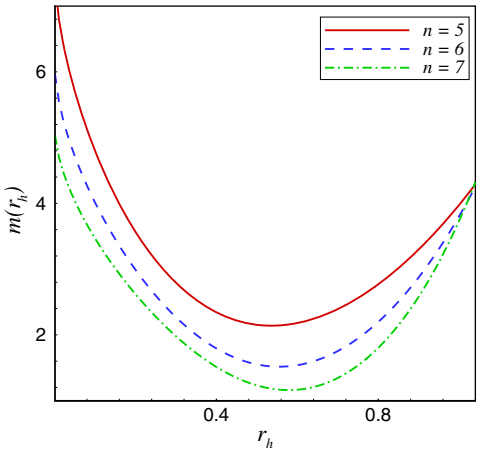

FIG. 9 (color online). The mass parameter m versus r_h for $\alpha = 0.5$, $q = 1$ and $\beta = 2$.

simplicity, in these figures, we set $l = b = 1$. If the line $m = \text{const}$ can cut the curve $m(r_h)$ just for one r_h, we have an extremal black hole. In this case, m has the extremal value m_{ext}, like the curve ($m = 2.9$) [m_{ext} is the minimum value of the curve $m(r_h)$]. For $m > m_{\text{ext}}$, the black hole has two horizons like the line ($m = 4$), and if $m < m_{\text{ext}}$, we have a naked singularity like the curve ($m = 1.6$). Looking at Fig. 8, it is clear that in the limit $r_h \to 0$, we have a nonzero value for the mass parameter $m(r_h)$. This is in contrast to the Schwarzschild black holes in which the mass parameter goes to zero as $r_h \to 0$. This contrast is due to the effect of the nonlinearity of the electrodynamic field. Figure 9 shows that m_{ext} decreases with an increase in the dimension of the spacetime.

IV. CONSERVED QUANTITY AND THERMODYNAMIC OF THE SOLUTIONS

In this section, we compute the conserved and thermodynamic quantities of the LNd black holes in all higher dimensions. We then also check the accuracy of the obtained thermodynamic quantities using the first law of black hole thermodynamics.

First, we obtain the charge of the mentioned black holes. According to Gauss's law, the electric charge of the black hole is

$$Q = \frac{1}{4\pi}\int_{r\to\infty} \exp[-4\alpha\Phi/(n-2)]^* F d\Omega = \frac{q\omega_{n-2}}{4\pi}, \quad (34)$$

where ω_{n-2} is the volume of a unit $(n-2)$-sphere. Another conserved quantity is the mass of the solutions. There are several ways for calculating the mass of the black holes. For example, for asymptotically AdS black holes, one can use the counterterm method inspired by AdS/CFT correspondence [38,39]. Another way for calculating the mass is through the use of the substraction method of Brown and York [40]. As we saw, due to the presence of the dilaton field, the asymptotic behavior of the solutions is neither flat nor (A)dS. In this case, the quasilocal formalism of Brown and York is sufficient to compute the quasilocal mass of a black hole. If we write the metric of spherically symmetric spacetime in the form [30]

$$ds^2 = -W^2(r)dt^2 + \frac{dr^2}{V^2(r)} + r^2 d\Omega_{n-2}^2, \quad (35)$$

and the matter action contains no derivatives of the metric, then the quasilocal mass is given by

$$\mathcal{M} = \frac{n-2}{2} r^{n-3} W(r)(V_0(r) - V(r)). \quad (36)$$

Here, $V_0(r)$ is an arbitrary function which determines the zero of the energy for a background spacetime and r is the

radius of the spacelike hypersurface boundary. If no cosmological horizon is present, the large r limit of (36) is used to determine the mass. For the obtained solutions, there is no cosmological horizon, and if we transform the metric to the form (35), then we obtain the mass of the black hole,

$$M = \frac{b^{(n-2)\gamma/2}(n-2)\omega_{n-2}}{16\pi(\alpha^2+1)}m. \tag{37}$$

In the absence of a nontrivial dilaton field ($\alpha = 0 = \gamma$), this expression for the mass reduces to the mass of the n-dimensional asymptotically AdS black hole.

Next, we calculate the temperature associated with the horizon of LNd black holes. The Hawking temperature of the black hole on the outer horizon r_+ may be obtained through the definition of surface gravity [4],

$$T_+ = \frac{\kappa}{2\pi} = \frac{1}{2\pi}\sqrt{-\frac{1}{2}(\nabla_\mu\chi_\nu)(\nabla^\mu\chi^\nu)}, \tag{38}$$

where κ is the surface gravity and $\chi = \partial/\partial t$ is the null Killing vector of the horizon. Taking $\chi^\nu = (-1, 0, 0, \ldots)$, we have $\chi_\nu = (f(r_+), 0, 0, \ldots)$ and hence $(\nabla_\mu\chi_\nu)(\nabla^\mu\chi^\nu) = -\frac{1}{2}[f'(r_+)]^2$, which leads to

$$\kappa = \sqrt{-\frac{1}{2}(\nabla_\mu\chi_\nu)(\nabla_\mu\chi_\nu)} = \frac{1}{2}\left(\frac{df(r)}{dr}\right)_{r=r_+}. \tag{39}$$

So the temperature of the charged dilaton black hole in the presence of the LN electrodynamics is obtained as

$$\begin{aligned} T_+ &= \frac{1}{4\pi}\left(\frac{df(r)}{dr}\right)_{r=r_+} \\ &= -\frac{\alpha^2+1}{4\pi}r_+^{1-\gamma}\left\{\frac{(n-3)b^{-\gamma}r_+^{2\gamma-2}}{\alpha^2-1} + \frac{2(\Lambda-4\beta^2)b^\gamma}{(n-2)}\right. \\ &\quad \left. + \frac{8\beta^2 b^\gamma}{n-2}\left[\sqrt{1+\eta_+} - \ln\left(\frac{\eta_+}{2}\right) + \ln\left(-1+\sqrt{1+\eta_+}\right)\right]\right\}, \end{aligned} \tag{40}$$

where $\eta_+ = \eta(r = r_+)$ and we have used $f(r_+) = 0$ for omitting m. For large β, we can expand T and arrive at

$$\begin{aligned} T_+ &= -\frac{(n-3)(\alpha^2+1)b^{-\gamma}}{4\pi(\alpha^2-1)}r_+^{\gamma-1} - \frac{\Lambda(\alpha^2+1)b^\gamma}{2\pi(n-2)}r_+^{1-\gamma} \\ &\quad - \frac{q^2(\alpha^2+1)b^{-\gamma(n-3)}}{2\pi(n-2)}r_+^{5-2n-3\gamma+n\gamma} \\ &\quad + \frac{q^4(\alpha^2+1)b^{-\gamma(2n-5)}}{16\pi(n-2)\beta^2}r_+^{9-4n-5\gamma+2n\gamma} + \mathcal{O}\left(\frac{1}{\beta^4}\right). \end{aligned} \tag{41}$$

In the limiting case where $\beta \to \infty$, the temperature reduces to the temperature of the higher-dimensional EMd black holes [31]. The behavior of T versus r_+ is shown in Figs. 10 and 11. Again, we fix $l = b = 1$, for simplicity. These figures show that for large values of r_+, each curve goes to a constant value independent of the model parameters. In Fig. 10, the temperature increases by increasing α. In Fig. 11, by increasing dimension n, the value of the temperature increases. The temperature of an extremal black hole is zero. We can obtain $r_{\rm ext}$ (the corresponding r for the extremal black hole) by solving $T_+ = 0$,

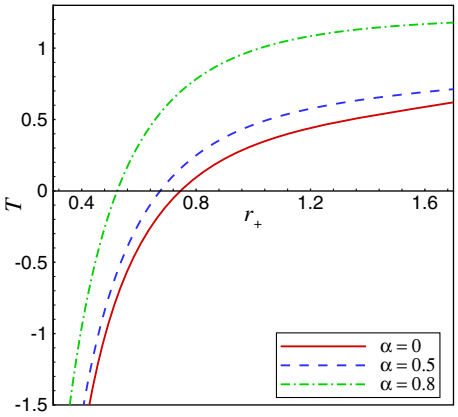

FIG. 10 (color online). The temperature T versus r_+ for different values of α. Here, we take $q = 2$, $n = 5$ and $\beta = 1$.

$$\begin{aligned} &\frac{(n-3)b^{-\gamma}r_{\rm ext}^{2\gamma-2}}{\alpha^2-1} + \frac{2(\Lambda-4\beta^2)b^\gamma}{(n-2)} \\ &+ \frac{8\beta^2 b^\gamma}{n-2}\left[\sqrt{1+\eta_{\rm ext}} + \ln\left(\frac{\eta_{\rm ext}}{2}\right) + \ln\left(-1+\sqrt{1+\eta_{\rm ext}}\right)\right] = 0. \end{aligned} \tag{42}$$

So $r_{\rm ext}$ is the positive root of the above equation, where

$$\eta_{\rm ext} \equiv \frac{q_{\rm ext}^2 r_{\rm ext}^{(n-2)(\gamma-2)}}{\beta^2 b^{(n-2)\gamma}}. \tag{43}$$

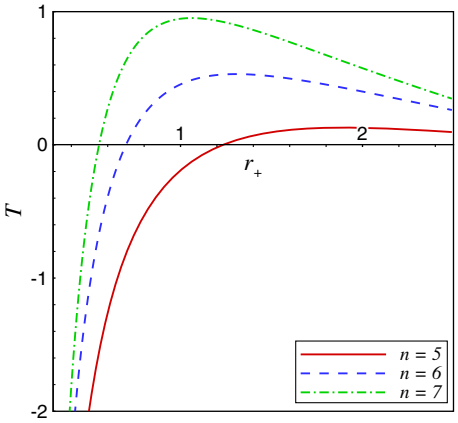

FIG. 11 (color online). The temperature T versus r_+ for different values of dimension n. Here, we take $\alpha = 2$, $q = 3$ and $\beta = 1$.

Also, we see that, for $r > r_{\rm ext}$, the temperature is positive ($T > 0$). In this case, the black hole has two horizons, r_- and r_+. For $r < r_{\rm ext}$, the temperature is negative ($T < 0$), and we encounter a naked singularity. It is notable that the value of $r_{\rm ext}$ depends on the other parameters and alters by changing the metric parameters.

Next, we calculate the electric potential. For this purpose, we use the definition $F_{\mu\nu} = \partial_\mu A_\nu - \partial_\nu A_\mu$, where $F_{\mu\nu}$ is the electromagnetic field tensor and A_μ is the corresponding gauge potential. For the static solution, all components of $F_{\mu\nu}$ are zero, except F_{tr} which is given by (30). This implies that $F_{tr} = \partial_t A_r - \partial_r A_t$, and the gauge potential is only a function of r, namely, $A_t = A_t(r)$, which is obtained as

$$A_t(r) = -\int F_{tr} dr = -\int \frac{2qb^{(4-n)\gamma/2}}{r^{n-2+2\gamma-n\gamma/2}} \times \frac{1}{1+\sqrt{1+\eta}} dr, \quad (44)$$

where η is defined in (21). Integrating (44) yields

$$A_t = \frac{q(\alpha^2+1)b^{(4-n)\gamma/2}}{\alpha^2+n-3} r^{3-n-(4-n)\gamma/2} \times {}_3F_2\left(\left[\frac{1}{2}, 1, \frac{3-n-\alpha^2}{4-2n}\right], \left[2, \frac{7-3n-\alpha^2}{4-2n}\right], -\eta\right), \quad (45)$$

where ${}_3F_2$ is the hypergeometric function and we have set the constant of integration equal to zero. The electric potential U is $A_\mu \chi^\mu$ at infinity with respect to the horizon [26],

$$U = A_\mu \chi^\mu|_{r\to\infty} - A_\mu \chi^\mu|_{r=r_+}, \quad (46)$$

where $\chi = \partial_t$ is the null generator of the horizon. Therefore, the electric potential is

$$U = \frac{q(\alpha^2+1)b^{(4-n)\gamma/2}}{\alpha^2+n-3} r_+^{3-n-(4-n)\gamma/2} \times F\left(\left[\frac{1}{2}, 1, \frac{3-n-\alpha^2}{4-2n}\right], \left[2, \frac{7-3n-\alpha^2}{4-2n}\right], -\eta_+\right). \quad (47)$$

Expanding for large values of β, we arrive at

$$U = \frac{q(\alpha^2+1)b^{(4-n)\gamma/2}}{(\alpha^2+n-3)r_+^{n-3+2\gamma-n\gamma/2}} + \mathcal{O}\left(\frac{1}{\beta^2}\right), \quad (48)$$

which is the electric potential of the higher-dimensional EMd black holes [31]. The behavior of the electric potential U as a function of horizon radius r_+ is displayed in Figs. 12 and 13 for $b = 1$. In both figures, U goes to zero for large values of r_+ independent of the model parameters. In Fig. 12, for special values of α the value of U is finite in the limit $r_+ \to 0$. This is the other proof of the success of nonlinear theory. By increasing the value of α, U goes to infinity. Also in Fig. 13, up to a certain value of parameter β, nonlinear electrodynamics could cancel the divergency and cause finite values at the origin. By increasing the value of β, the divergency returns and the curve comes closer to the electric potential of EMd black holes.

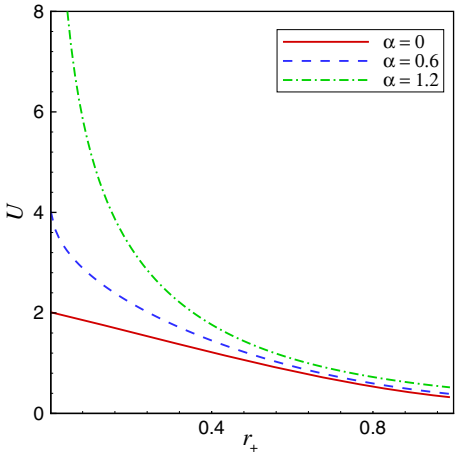

FIG. 12 (color online). The electric potential U versus r_+ for $q = 1$, $b = 1$, $\beta = 1$ and $n = 6$ and different α.

To obtain entropy of the LNd black hole, we use the so-called area law of entropy. This law states that the entropy of the black hole is a quarter of the event horizon area [41]. This near universal law applies to almost all kinds of black holes, including dilaton black holes, in Einstein gravity [42]. The entropy of the black hole can be calculated as

$$S = \frac{b^{(n-2)\gamma/2} r_+^{(n-2)(1-\gamma/2)} \omega_{n-2}}{4}. \quad (49)$$

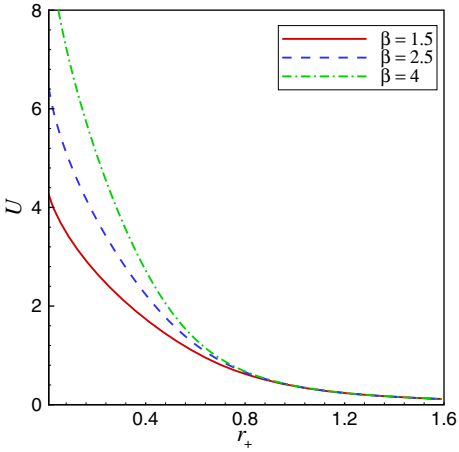

FIG. 13 (color online). The electric potential U versus r_+ for $b = 1$, $\alpha = 0.5$, $n = 6$ and $q = 1$ and different β.

After calculating thermodynamic quantities, we are now in a position to check the first law of thermodynamics. In order to do this, we obtain m by solving $f(r_+)=0$, and replace it in the mass expression (37) of the black hole. Then, by using Eqs. (34) and (49), we obtain the mass M as a function of extensive quantities S and Q,

$$\begin{aligned}M(S,Q)=&-\frac{(n-2)(n-3)(\alpha^2+1)b^{-\alpha^2}(4S)^{\frac{\alpha^2+n-3}{n-2}}}{16\pi(\alpha^2-1)(\alpha^2+n-3)}+\frac{(\Lambda-4\beta^2)(\alpha^2+1)b^{\alpha^2}(4S)^{\frac{-\alpha^2+n-1}{n-2}}}{8\pi(\alpha^2-n+1)}\\&+\frac{(n-2)\beta^2(\alpha^2+1)b^{\alpha^2}}{2\pi(\alpha^2-n+1)^2}(4S)^{\frac{-\alpha^2+n-1}{n-2}}\left\{1-{}_2F_1\left(\left[\frac{-1}{2},\frac{\alpha^2-n+1}{2n-4}\right],\left[\frac{\alpha^2+n-3}{2n-4}\right],-\zeta\right)\right\}\\&+\frac{\beta^2(\alpha^2+1)b^{\alpha^2}}{2\pi(\alpha^2-n+1)}(4S)^{\frac{-\alpha^2+n-1}{n-2}}\left\{\sqrt{1+\zeta}-\ln\left(\frac{\zeta}{2}\right)+\ln(-1+\sqrt{1+\zeta})\right\},\end{aligned}\tag{50}$$

where $\zeta=\frac{\pi^2Q^2}{S^2\beta^2}$. If we expand $M(S,Q)$ for large β, we get

$$\begin{aligned}M(S,Q)=&-\frac{(n-2)(n-3)(\alpha^2+1)b^{-\alpha^2}}{16\pi(\alpha^2-1)(\alpha^2+n-3)}(4S)^{\frac{\alpha^2+n-3}{n-2}}+\frac{\Lambda(\alpha^2+1)b^{\alpha^2}}{8\pi(\alpha^2-n+1)}(4S)^{\frac{-\alpha^2+n-1}{n-2}}\\&+\frac{2\pi Q^2(\alpha^2+1)b^{\alpha^2}}{\alpha^2+n-3}(4S)^{\frac{\alpha^2+n-3}{2-n}}-\frac{4\pi^3Q^4(\alpha^2+1)b^{\alpha^2}}{\beta^2(\alpha^2+3n-7)}(4S)^{\frac{-\alpha^2-3n+7}{n-2}}+\mathcal{O}\left(\frac{1}{\beta^4}\right),\end{aligned}\tag{51}$$

which is exactly the Smarr-type formula obtained for EMd black holes in the limit $\beta\to\infty$ [31]. One may then regard the parameters S and Q as a complete set of extensive parameters for the mass $M(S,Q)$. So we can define their related intensive parameters S and Q as

$$T=\left(\frac{\partial M}{\partial S}\right)_Q,\qquad U=\left(\frac{\partial M}{\partial Q}\right)_S.\tag{52}$$

Numerical calculations show that the intensive quantities calculated by Eq. (52) coincide with Eqs. (40) and (47). Thus, our obtained thermodynamic quantities obey the first law of black hole thermodynamics,

$$dM=TdS+UdQ.\tag{53}$$

The ability of the mentioned theory to remove the divergency of the electric field at the origin, reducing all the obtained quantities in the limit $\beta\to\infty$ to the known results in the literature [31,35], and finally the correction of the obtained quantities in the frame of the first law of black hole thermodynamics all confirm the truth of our calculation. Our results are also in agreement with other methods such as the Euclidean action method [43].

V. THERMODYNAMIC STABILITY IN CANONICAL ENSEMBLE

The other interesting and necessary subject for studying black holes is investigating the thermal stability in different ensembles. The stability of a thermodynamic system is determined by analyzing the behavior of the entropy $S(M,Q)$ with respect to small variations of the thermodynamic coordinates around the equilibrium. The local stability in any ensemble requires that $S(M,Q)$ be a concave function of the intensive variables. The energy $M(S,Q)$ is also another parameter for investigating stability which should be a convex function of its extensive variable. Therefore, by finding the determinant of the Hessian matrix of $M(S,Q)$ with respect to its extensive variables X_i, $H^M_{X_iX_j}=[\partial^2M/\partial X_i\partial X_j]$, we can study the local stability [44,45]. The number of X_i depends on the ensemble that is used. In the canonical ensemble, the charge is a fixed parameter, and thus the positivity of the heat capacity guarantees the local stability. The heat capacity is defined as

$$C_Q=T\left(\frac{\partial S}{\partial T}\right)_Q=T\left(\frac{\partial^2M}{\partial S^2}\right)^{-1}_Q.\tag{54}$$

The negative temperature is not physically accepted, so the required condition for the local stability is the positivity of T and $(\partial^2M/\partial S^2)_Q$, simultaneously. In order to find the stable region for the corresponding black hole in the canonical ensemble, we have plotted $(\partial^2M/\partial S^2)_Q$ and temperature versus α for different values of q in Figs. 14–16. We have fixed $l=b=1$ in these figures. As one can see from Figs. 14(a), 15(a) and 16(a), there is a $q_{\min}$ for which $(\partial^2M/\partial S^2)_Q$ are positive for all values of α provided $q>q_{\min}$. For $q<q_{\min}$, there is an $\alpha_{\max}$ for which $(\partial^2M/\partial S^2)_Q$ are positive for $\alpha<\alpha_{\max}$, while they are negative for $\alpha>\alpha_{\max}$. By increasing n, the value of $q_{\min}$ becomes larger, which indicates that the region of stability becomes smaller. Also, for every $q<q_{\min}$, the value of $\alpha_{\max}$ decreases, so the region of stability becomes smaller.

In Figs. 14(b), 15(b) and 16(b), we see that, for $\alpha<1$ and the lowest dimension ($n=4$), there is a $q_1^{\min}$ in which

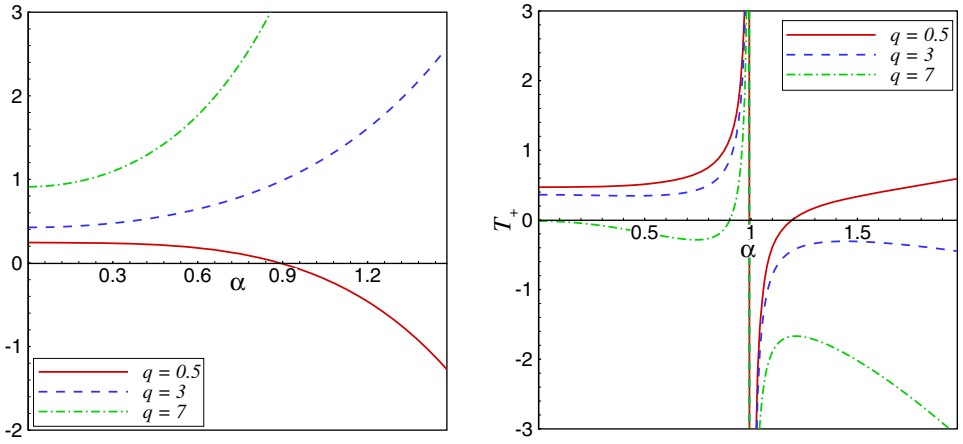

(a) $\left(\partial^2 M/\partial S^2\right)_Q$ versus α (b) Temperature versus α

FIG. 14 (color online). Thermal stability in the canonical ensemble for $\beta = 1$, $r_+ = 1.8$ and $n = 4$.

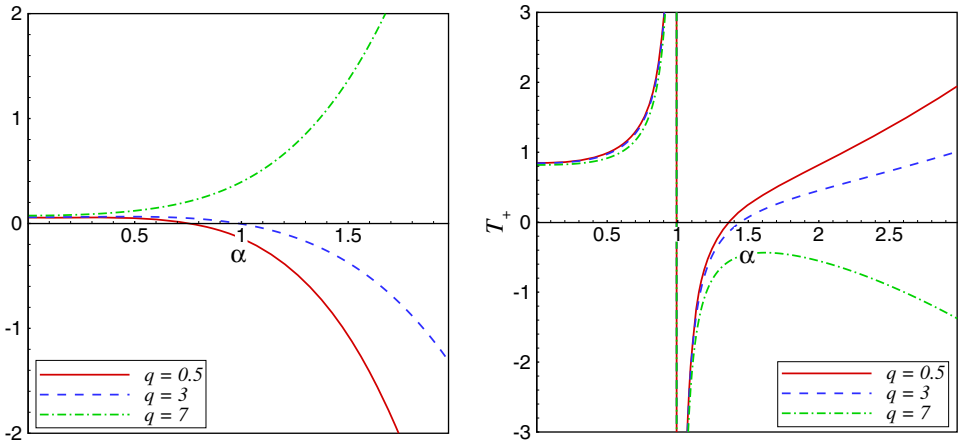

(a) $\left(\partial^2 M/\partial S^2\right)_Q$ versus α (b) Temperature versus α

FIG. 15 (color online). Thermal stability in the canonical ensemble for $\beta = 1$, $r_+ = 1.8$ and $n = 6$.

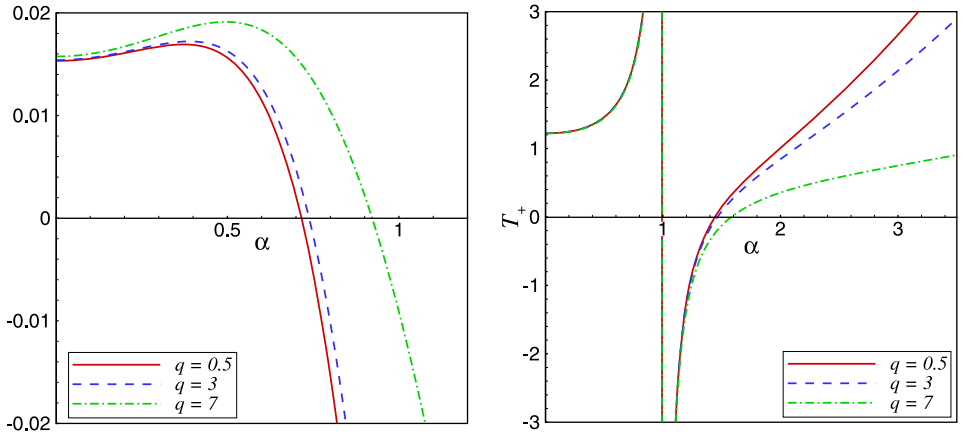

(a) $\left(\partial^2 M/\partial S^2\right)_Q$ versus α (b) Temperature versus α

FIG. 16 (color online). Thermal stability in the canonical ensemble for $\beta = 1.5$, $r_+ = 1.8$ and $n = 8$.

for $q > q_1^{\min}$, the temperature is negative, while the temperature is positive for $q < q_1^{\min}$. By increasing n, T is positive for all values of q and $\alpha < 1$. For $\alpha > 1$, there is a $q_2^{\min}$ for which the temperature is negative for $q > q_2^{\min}$ and all values of α. For $q < q2_{\min}$, there is an $\alpha_{\min}$ in which the temperature is negative for $\alpha < \alpha_{\min}$ and positive for $\alpha > \alpha_{\min}$. By increasing the dimension n, the value of $q_2^{\min}$ increases.

VI. THERMODYNAMIC STABILITY IN GRAND-CANONICAL ENSEMBLE

In this section, we investigate thermal stability in the grand-canonical ensemble. In this ensemble, both charge Q and entropy S are thermodynamic variables. Therefore, in the ranges of the parameter spaces where the determinant of the Hessian matrix H, the two diagonal elements of H, and the temperature are positive, we have local stability. The Hessian matrix is $\binom{H_{11}\ H_{12}}{H_{21}\ H_{22}}$, and the components of its determinant are

$$H_{11} = \left(\frac{\partial^2 M}{\partial S^2}\right)_Q, \qquad H_{22} = \left(\frac{\partial^2 M}{\partial Q^2}\right)_S,$$
$$H_{21} = H_{12} = \left(\frac{\partial^2 M}{\partial S \partial Q}\right). \tag{55}$$

Since the above components are too long, for economical reasons, we do not use them here. It is important to note that in the canonical ensemble, the system is thermally stable provided $T > 0$, $(\partial^2 M/\partial S^2)_Q > 0$, and

$$\det(H) = \left(\frac{\partial^2 M}{\partial S^2}\right)_Q \left(\frac{\partial^2 M}{\partial Q^2}\right)_S - \left(\frac{\partial^2 M}{\partial S \partial Q}\right)^2 > 0. \tag{56}$$

Thus,

$$\left(\frac{\partial^2 M}{\partial Q^2}\right)_S > \left(\frac{\partial^2 M}{\partial S \partial Q}\right)^2 \Big/ \left(\frac{\partial^2 M}{\partial S^2}\right)_Q > 0. \tag{57}$$

This clearly shows that the positivity of $\det(H)$ and $(\partial^2 M/\partial S^2)_Q$ leads to $(\partial^2 M/\partial Q^2)_S > 0$. In order to study the stability, we have plotted the determinant of the Hessian matrix and temperature versus β for different q in Figs. 17–18. Again, we choose $l = b = 1$ for simplicity. From Fig. 17(a), we see that for the lowest dimension $n = 4$, the determinant is positive for all values of q and $\alpha = 0.5$ ($\alpha < 1$). In Fig. 17(b), the temperature is positive for small q and all values of β. For large q, there is a $\beta_{\max}$ for which the temperature is positive for $\beta < \beta_{\max}$ and negative for $\beta > \beta_{\max}$. From Fig. 18, we see that for higher dimensions ($n = 7$) and $\alpha < 1$, the Hessian matrix determinant and the temperature are positive for $\alpha = 0.5$, $r_+ = 1.5$.

VII. PHASE TRANSITION POINTS AND SINGULARITIES OF THERMODYNAMIC GEOMETRY

Another interesting subject for studying black hole physics is the geometry approach towards thermodynamics. Weinhold was the first to introduce, in equilibrium space, a Riemannian metric defined in terms of the second derivatives of the internal energy with respect to entropy and other extensive variables of a thermodynamic system [46,47]. Then, Ruppeiner introduced another metric defined as the negative Hessian of entropy with respect to the internal energy and other extensive quantities of a thermodynamic system [48,49]. The Ruppeiner metric is conformally related to the Weinhold metric with the inverse temperature as the conformal factor [50],

$$dS_R^2 = \frac{dS_W^2}{T}. \tag{58}$$

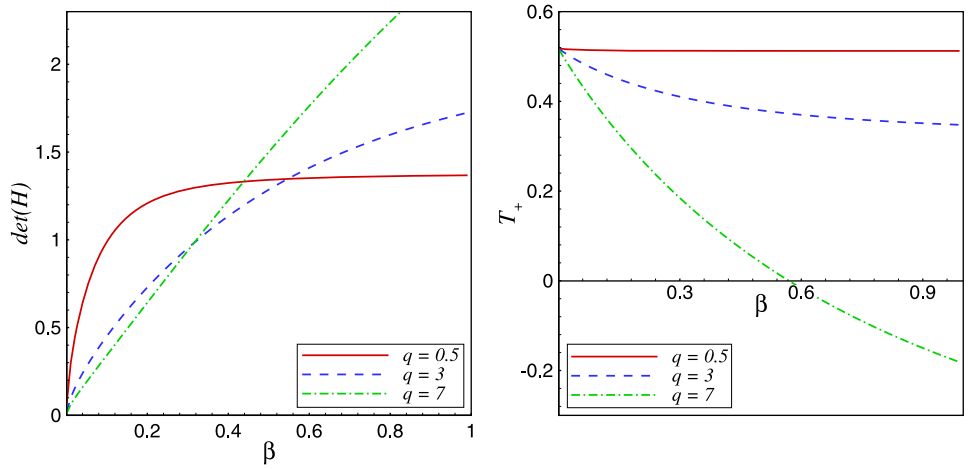

(a) $det(H)$ versus β (b) Temperature versus β

FIG. 17 (color online). Thermal stability in the grand-canonical ensemble for $\alpha = 0.5$, $r_+ = 1.8$ and $n = 4$.

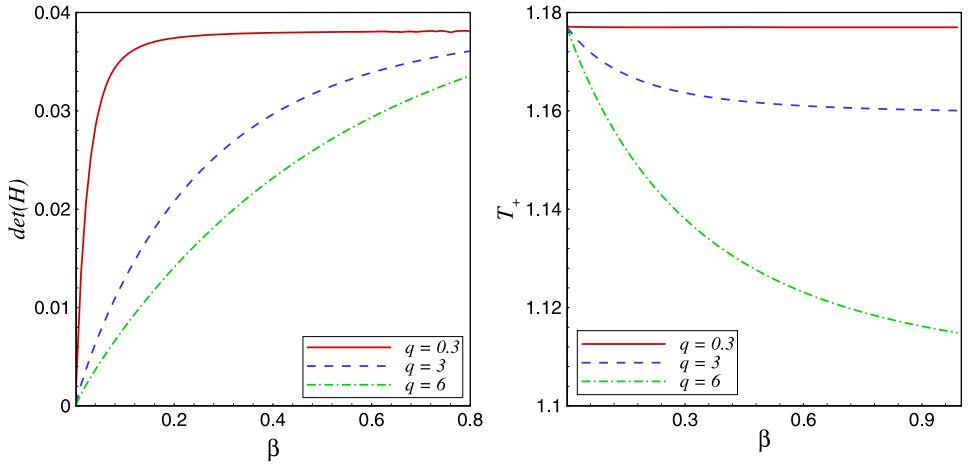

(a) $det(H)$ versus β (b) Temperature versus β

FIG. 18 (color online). Thermal stability in the grand-canonical ensemble for $\alpha = 0.5$, $r_+ = 1.5$ and $n = 7$.

Weinhold or Ruppeiner metrics have an unavoidable problem. In equilibrium space, their results depend on the choice of thermodynamic potential; i.e., the results are not invariant with respect to Legendre transformations. After this problem, a possible solution was suggested by Quevedo whose starting point was the observation that standard thermodynamics is invariant with respect to Legendre transformations [51–54]. Quevedo's metric also had some problems. Sometimes, the divergency points of the Ricci scalar are not the same as the phase transition points, and sometimes, the Ricci scalar diverges at a point where we have no phase transition. In summary, the thermodynamical Ricci scalars of Weinhold, Ruppeiner and Quevedo metrics have some problems, and their number and location of divergences do not coincide with phase transition points arising from heat capacity. In order to solve this problem, a new approach toward a geometrical concept of black hole thermodynamics was proposed by Hendi *et al.* [55]. It was argued that the denominator of the Ricci scalar of the new metric contains terms which coincide with different types of phase transitions. In this section, employing the metric of [55,56], we show that the phase transition points (the points at which heat capacity is zero or diverges) happen at the points where the Ricci scalar diverges. This metric is written as [55,56]

$$ds^2 = S\frac{M_S}{M_{QQ}^3}(-M_{SS}dS^2 + M_{QQ}dQ^2). \tag{59}$$

Using metric (59), we first calculate the Ricci scalar R. Then, we plot the Ricci scalar, the heat capacity C_Q and the temperature versus r_+ in Figs. 19–20. For simplicity, we choose $l = 1$ and $b = 2$. In Fig. 19, we have plotted R, C_Q and T versus r_+ for $\alpha < 1$ and different values of dimension n. As one can see in Figs. 19(a), 19(b) and 19(c), there is a phase transition point in which the Ricci scalar R diverges, while the heat capacity C_Q is zero. In this kind of phase transition, the black hole changes its behavior from an unreal case to a real case. In these figures, the temperature is not negative, so these phase transition points

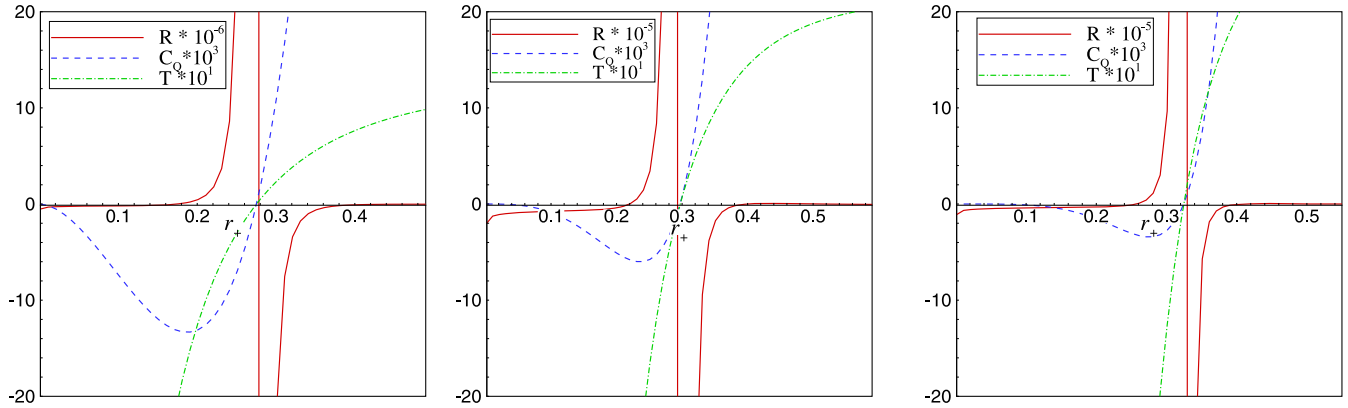

(a) $n = 5$ (b) $n = 7$ (c) $n = 9$

FIG. 19 (color online). Ricci scalar R, heat capacity C_Q and temperature T versus r_+ for $\alpha = 0.8$, $\beta = 1$ and $q = 1$.

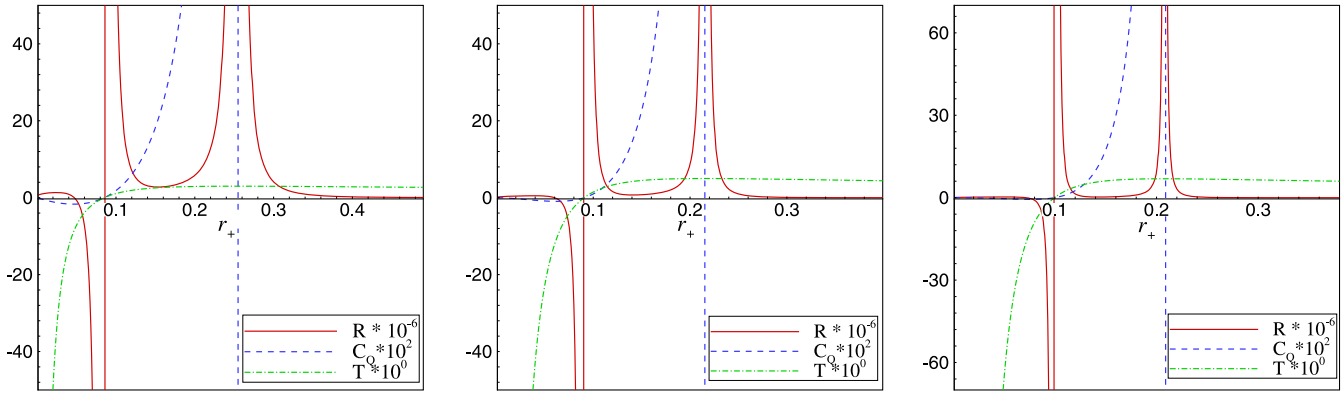

(a) $n = 5$ (b) $n = 7$ (c) $n = 9$

FIG. 20 (color online). Ricci scalar R, heat capacity C_Q and temperature T versus r_+ for $\alpha = 1.4$, $\beta = 1$ and $q = 1$.

are physical. By increasing the value of n, the r_+ of the related phase transition points becomes larger.

In Fig. 20, we have investigated the phase transition points for $\alpha > 1$ and different values of n. As we can see, by increasing the value of α, the number of phase transition points increases with respect to the case $\alpha < 1$. In these figures, there are two phase transition points in which the Ricci scalar goes to infinity, while the heat capacity goes to zero for the first point and to ∞ for the second one. The temperature is zero for the first point and has a finite value for the second one. By increasing n, the r_+ of the two phase transition points get closer to each other.

VIII. CONCLUDING REMARKS

The motivation for investigating the nonlinear electrodynamics is to remove the divergency of the electric field of a pointlike charged particle located at the origin in Maxwell theory. In this paper, we considered LN electrodynamics in all higher dimensions by taking into account the dilaton scalar field in the action. By varying the action, we found the field equations governing the evolution of the gravitational field, the dilaton field and the nonlinear gauge field. Then, we constructed a new class of static and spherically symmetric black hole solutions of this theory. Probing the electric field, we understood that the LN electrodynamics could lead to a finite value at the origin for the electric field in the absence of the dilaton field ($\alpha = 0 = \gamma$).

In all steps, for $\beta \to \infty$ our solutions restore the higher-dimensional EMd black hole solutions, while in the absence of the dilaton field ($\alpha = 0\gamma$), they reduce to the dilaton black holes coupled to EN electrodynamics. Also, we understood that in the presence of the dilaton field, the asymptotic behavior of the metric is neither flat nor (A)dS. We also studied the casual structure of the solutions. Depending on the different parameters, we may have a black hole with two horizons, an extremal black hole or a naked singularity. Then, we calculated the conserved and thermodynamic quantities such as the mass, temperature and the electric potential. For the fixed values of the parameters β, q and n, we have a black hole with two horizons provided $T > 0$, an extremal black hole for $T = 0$ and a naked singularity if $T < 0$. Using the Smarr-type formula, we checked the correction of the first law of black hole thermodynamics in all higher dimensions. We also investigated thermal stability in the canonical and grand-canonical ensembles. We found that in both ensembles, the system is thermally stable for small α independent of the other parameters. Indeed, in both the canonical and grand-canonical ensembles, the black holes are stable provided $\alpha < 1$, while for $\alpha > 1$ the system may have an unstable phase. By increasing n, the region of stability for α becomes smaller but we have stability for all values of q.

We also studied thermodynamical geometry by using the new metric proposed in [55]. We found the phase transition points of this metric by considering the Ricci scalar. We have shown that for $\alpha < 1$, we have just one phase transition point which becomes larger by increasing n. In this kind of phase transition, the black hole changes its behavior from an unreal case to a real case. For $\alpha > 1$, there are two phase transition points in which the Ricci scalar goes to infinity, while the heat capacity goes to zero for the first point and it goes to ∞ for the second one. The temperature is zero for the first point, and it has a finite value for the second one. By increasing the dimension of spacetime, n, the two points get closer to each other. We found that, depending on the values of the parameters α, β and q, the obtained black hole solutions have different behavior. We showed that for small α and β, we have black holes which are thermally stable. Indeed, for $\alpha < 0.5$ and $\beta < 0.5$, the mentioned black holes are thermally stable with physical temperatures for the arbitrary values of the charge parameter q, and the electric field and electric potential also have finite values at the origin for these ranges of the parameters.

Finally, we mention that, in this work, we only considered the static and spherically symmetric black holes of LNd theory. Therefore, it is interesting to extend the study to the rotating black holes or branes and explore their thermodynamics as well as thermodynamic geometry of the stationary black holes in the presence of LNd electrodynamics.

ACKNOWLEDGMENTS

We thank the referee for constructive comments which helped us improve the paper significantly. We also thank the Shiraz University Research Council. The work of A. S. has been supported financially by the Research Institute for Astronomy and Astrophysics of Maragha, Iran.

[1] M. Born and L. Infeld, Proc. R. Soc. A **144**, 425 (1934).
[2] E. Fradkin and A. Tseytlin, Phys. Lett. B **163B**, 123 (1985); R. Matsaev, M. Rahmanov, and A. Tseytlin, Phys. Lett. B **193**, 205 (1987); E. Bergshoeff, E. Sezgin, C. Pope, and P. Townsend, Phys. Lett. B **188**, 70 (1987).
[3] C. Callan, C. Lovelace, C. Nappi, and S. Yost, Nucl. Phys. **B308**, 221 (1988); O. Andreev and A. Tseytlin, Nucl. Phys. **B311**, 221 (1988); R. Leigh, Mod. Phys. Lett. A **04**, 2767 (1989).
[4] S. H. Hendi, J. High Energy Phys. 03 (2012) 065; S. H. Hendi and A. Sheykhi, Phys. Rev. D **88**, 044044 (2013).
[5] M. Hassaine, J. Math. Phys. (N.Y.) **47**, 033101 (2006).
[6] H. H. Soleng, Phys. Rev. D **52**, 6178 (1995).
[7] M. B. Green, J. H. Schwarz, and E. Witten, *Superstring Theory* (Cambridge University Press, Cambridge England, 1987).
[8] R. Gregory and J. A. Harvey, Phys. Rev. D **47**, 2411 (1993).
[9] G. W. Gibbons and K. Maeda, Ann. Phys. (N.Y.) **167**, 201 (1986).
[10] J. H. Horne and G. T. Horowitz, Phys. Rev. D **46**, 1340 (1992).
[11] A. Sheykhi and S. Hajkhalili, Phys. Rev. D **89**, 104019 (2014).
[12] S. Abdolrahimi and A. A. Shoom, Phys. Rev. D **83**, 104023 (2011).
[13] S. J. Poletti and D. L. Wiltshire, Phys. Rev. D **50**, 7260 (1994); S. J. Poletti, J. Twamley, and D. L. Wiltshire, Phys. Rev. D **51**, 5720 (1995); S. Mignemi and D. L. Wiltshire, Phys. Rev. D **46**, 1475 (1992).
[14] L. Randallt and R. Sundrum, Phys. Rev. Lett. **83**, 3370 (1999).
[15] G. Dvali, G. Gabadadze, and M. Porrati, Phys. Lett. B **485**, 208 (2000).
[16] O. Aharony, S. S. Gubser, J. M. Maldacena, H. Ooguri, and Y. Oz, Phys. Rep. **323**, 183 (2000).
[17] T. Tamaki and T. Torii, Phys. Rev. D **62**, 061501(R) (2000).
[18] T. Tamaki and T. Torii, Phys. Rev. D **64**, 024027 (2001).
[19] R. Yamazaki and D. Ida, Phys. Rev. D **64**, 024009 (2001).
[20] S. S. Yazadjiev, Phys. Rev. D **72**, 044006 (2005).
[21] G. Clement and D. Gal'tsov, Phys. Rev. D **62**, 124013 (2000).
[22] S. S. Yazadjiev, P. P. Fiziev, T. L. Boyadjiev, and M. D. Todorov, Mod. Phys. Lett. A **16**, 2143 (2001).
[23] A. Sheykhi, N. Riazi, and M. H. Mahzoon, Phys. Rev. D **74**, 044025 (2006).
[24] A. Sheykhi and N. Riazi, Phys. Rev. D **75**, 024021 (2007); A. Sheykhi, Int. J. Mod. Phys. D **18**, 25 (2009).
[25] A. Sheykhi, Phys. Lett. B **662**, 7 (2008).
[26] M. H. Dehghani, S. H. Hendi, A. Sheykhi, and H. R. Sedehi, J. Cosmol. Astropart. Phys. 02 (2007) 020; M. H. Dehghani, A. Sheykhi, and S. H. Hendi, Phys. Lett. B **659**, 476 (2008).
[27] A. Sheykhi and A. Kazemi, Phys. Rev. D **90**, 044028 (2014).
[28] M. K. Zangeneh, A. Sheykhi, and M. H. Dehghani, Phys. Rev. D **91**, 044035 (2015); **92**, 024050 (2015); Eur. Phys. J. C **75**, 497 (2015).
[29] A. Sheykhi, F. Naeimipour, and S. M. Zebarjad, Phys. Rev. D **91**, 124057 (2015).
[30] K. C. K. Chan, J. H. Horne, and R. B. Mann, Nucl. Phys. **B447**, 441 (1995).
[31] A. Sheykhi, Phys. Rev. D **76**, 124025 (2007).
[32] R. G. Cai, J. Y. Ji, and K. S. Soh, Phys. Rev. D **57**, 6547 (1998); R. G. Cai and Y. Z. Zhang*ibid.* **64**, 104015 (2001).
[33] S. S. Yazadjiev, Classical Quantum Gravity **22**, 3875 (2005).
[34] G. Clement, D. Gal'tsov, and C. Leygnac, Phys. Rev. D **67**, 024012 (2003); G. Clement and C. Leygnac, *ibid.* **70**, 084018 (2004).
[35] S. H. Hendi, Ann. Phys. (Amsterdam) **333**, 282 (2013).
[36] M. H. Dehghani and N. Farhangkhah, Phys. Rev. D **71**, 044008 (2005).
[37] M. Abramowitz and I. A. Stegun, *Handbook of Mathematical Functions* (Dover, New York, 1972); R. M. Corless, G. H. Gonnet, D. E. G. Hare, D. J. Jeffrey, and D. E. Knuth, Adv. Comput. Math. **5**, 329 (1996).
[38] J. Maldacena, Adv. Theor. Math. Phys. **2**, 231 (1998); E. Witten, *ibid.* **2**, 253 (1998); O. Aharony, S. S. Gubser, J. Maldacena, H. Ooguri, and Y. Oz, Phys. Rep. **323**, 183 (2000); V. Balasubramanian and P. Kraus, Commun. Math. Phys. **208**, 413 (1999).
[39] S. de Haro, K. Skenderis, and S. N. Solodukhin, Commun. Math. Phys. **217**, 595 (2001).
[40] J. Brown and J. York, Phys. Rev. D **47**, 1407 (1993); J. D. Brown, J. Creighton, and R. B. Mann, Phys. Rev. D **50**, 6394 (1994).
[41] J. D. Beckenstein, Phys. Rev. D **7**, 2333 (1973); S. W. Hawking, Nature (London) **248**, 30 (1974); G. W. Gibbons and S. W. Hawking, Phys. Rev. D **15**, 2738 (1977).
[42] C. J. Hunter, Phys. Rev. D **59**, 024009 (1998); S. W. Hawking, C. J. Hunter, and D. N. Page*ibid.* **59**, 044033 (1999); R. B. Mann*ibid.* **60**, 104047 (1999); **61**, 084013 (2000).

[43] O. Miskovic and R. Olea, Phys. Rev. D **77**, 124048 (2008).
[44] M. Cvetic and S. S. Gubser, J. High Energy Phys. 04 (1999) 024; M. M. Caldarelli, G. Cognola, and D. Klemm, Classical Quantum Gravity **17**, 399 (2000).
[45] S. S. Gubser and I. Mitra, J. High Energy Phys. 08 (2001) 018.
[46] F. Weinhold, J. Chem. Phys. **63**, 2479 (1975).
[47] F. Weinhold, J. Chem. Phys. **63**, 2484 (1975).
[48] G. Ruppeiner, Phys. Rev. A **20**, 1608 (1979).
[49] G. Ruppeiner, Rev. Mod. Phys. **67**, 605 (1995); **68**, 313(E) (1996).
[50] P. Salamon, J. D. Nulton, and E. Ihrig, J. Chem. Phys. **80**, 436 (1984).
[51] H. Quevedo, J. Math. Phys. (N.Y.) **48**, 013506 (2007).
[52] H. Quevedo, Gen. Relativ. Gravit. **40**, 971 (2008).
[53] H. Quevedo, A. Sanchez, S. Taj, and A. Vazquez, Gen. Relativ. Gravit. **43**, 1153 (2011).
[54] H. Quevedo, Gen. Relativ. Gravit. **40**, 971 (2008).
[55] S. H. Hendi, S. Panahiyan, B. Eslam Panah, and M. Momennia, Eur. Phys. J. C **75**, 507 (2015).
[56] S. H. Hendi, A. Sheykhi, S. Panahiyan, and B. Eslam Panah, Phys. Rev. D **92**, 064028 (2015).